Studies in Applied Mathematics, Vol. LII, No. 1, March 1973.

The Static-Geometric Duality and a Staggered Mesh Scheme in the Numerical Solution of Some Shell Problems*

By R. L. Mallett and F. Y. M. Wan

1. Introduction

We are concerned here with the numerical solution of two problems for elastic helicoidal shells. The following unusual computational features of these problems are of interest:

(1) The two seemingly unrelated physical problems are seen to give rise to the same mathematical problem once we establish a complete static geometric duality between them, *boundary conditions included.*

(2) The relevant boundary value problem is associated with a *sixth* order system of differential equations which is not at all typical within the framework of a first approximation shell theory.

(3) A certain difficulty in connection with a numerical solution of the boundary value problem is resolved with the help of a *staggered mesh* finite difference scheme.

More specifically, we consider right helicoidal shells (with middle surface equation $z = a\theta$) with stress resultants (N, Q), stress couples (M), midsurface strains (ε), curvature changes (κ, λ) and surface loads (p) (and edge loads) of the form

$$
\begin{aligned}
&(N_r, N_\theta, Q_\theta, M_{r\theta} = M_{\theta r}, \varepsilon_r, \varepsilon_\theta, \kappa_{\theta r}, \kappa_{r\theta}, \lambda_r, p_r) \\
&\qquad = (n_r, n_\theta, q_\theta, m, e_r, e_\theta, k_{\theta r}, k_{r\theta}, l_r, P_r)\sin\theta \\
&(N_{r\theta}, N_{\theta r}, Q_r, M_r, M_\theta, \varepsilon_{r\theta} = \varepsilon_{\theta r}, \kappa_r, \kappa_\theta, \lambda_\theta, p_\theta, p_n) \\
&\qquad = (n_{r\theta}, n_{\theta r}, q_r, m_r, m_\theta, e, k_r, k_\theta, l_\theta, P_\theta, P_n)\cos\theta
\end{aligned}
\tag{1.1}
$$

where n_r, n_θ, etc. are functions of the radial coordinate r. In a more general formulation of linear shell theory as described in [6], λ_r and λ_θ are the normal components of the relevant curvature change vectors. For this class of stress and strain distributions, the differential equations of equilibrium, constitutivity and compatibility for elastic helicoidal shells can be satisfied identically by expressing the r-dependent part of the stress and strain measures in terms of a stress function $\psi(r)$ and a strain function $\phi(r)$ as given in [4]. $\psi(r)$ and $\phi(r)$ are then determined by two

* Preparation of this paper was partly supported by the Office of Naval Research under a contract with Massachusetts Institute of Technology.

coupled *third* order differential equations. Except for terms of order $h/R_{\min}$ (h is the shell thickness and $R_{\min}$ is the minimum radius of curvature), the two equations for a homogeneous and isotropic shell of constant thickness are

$$L(\psi) + \frac{a}{A}\phi = f_1(r), \qquad L^*(\phi) + \frac{a}{D}\psi = f_2(r) \tag{1.2}$$

where, in terms of Young's modulus, E, and Poisson's ratio $\nu\,(= \nu_s = \nu_b)$*,

$$A = \frac{1}{Eh}, \qquad D = \frac{Eh^3}{12(1-\nu_b^2)}.$$

$$L(\ ) = \alpha^3\frac{d^3(\ )}{dr^3} + 6r\alpha\frac{d^2(\ )}{dr^2} + \left[3 + (4+\nu_s)\frac{a^2}{\alpha^2}\right]\alpha\frac{d(\ )}{dr} - \left[3 + (5-\nu_s)\frac{a^2}{\alpha^2}\right]\frac{r}{\alpha}(\ ) \tag{1.3}$$

with $\alpha = (a^2 + r^2)^{1/2}$, and L^* obtained from L by replacing ν_s by $-\nu_b$. In the absence of surface load, the load terms f_1 and f_2 are given by

$$f_1(r) = P(3+\nu_s)\frac{a^3}{\alpha^3}, \qquad f_2(r) = k(3-\nu_b)\frac{a^3}{\alpha^3} \tag{1.4}$$

where P is the constant of integration in the first integral of the differential equations of equilibrium and k is the corresponding constant for the compatibility equations. They may be interpreted as the resultant side force per unit axial length and the curvature of the axis of the helicoid after deformation, respectively.

The equilibrium equations and compatibility equations for helicoidal shells with the specified polarly sinusoidal stress and strain distributions each have only one first integral. This contrasts with the corresponding class of problems for shells of revolution where each set of equations has two first integrals. Consequently, the system of differential equations is effectively a sixth order system in the case of helicoidal shells as indicated by (1.2), and only a fourth order system for shells of revolution [1, 12]. To the knowledge of the authors, there has not been any problem involving a genuine sixth order system of differential equations in a first approximation shell theory. In this paper, (1.2)–(1.4) will be used to solve the *pure bending* problem and the *side force* problem of helicoidal shells.

For the pure bending problem, the shell is free of surface load and free of edge traction along the two *helical edges*, $r = r_i$ and $r = r_0$, and is subject only to equal and opposite bending moments at the two *radial edges*, $\theta = \pm\theta_0$. The relationship between perturbation solutions of this problem for small and large values of the width-to-pitch ratio, $\lambda = r_0/a$, and the existing shallow shell solutions [5, 9] was

* We will continue to distinguish the two effective Poisson's ratios associated with the bending and stretching shell action even for a homogeneous and isotropic shell for ease of application of the static geometric duality.

discussed in [4]. An asymptotic solution for nonshallow but "sufficiently thin" shells was also obtained in [4] for moderate values of λ. For the range of values of λ and $\gamma = r_0/h$ not covered by these solutions, a finite difference solution is appropriate.

In the first part of this paper, we will show that the usual central difference scheme leads to an inconsistent finite difference analog of the differential equations (1.2). The use of this inconsistent analog would in turn lead to a solution scheme which is unstable. A consistent difference analog and a rapidly convergent (and stable) solution scheme will be obtained through the use of a staggered mesh. Numerical results for the overall bending stiffness and stress distributions will be obtained with the help of this finite difference scheme.

The second part of this paper deals with the formulation and method of solution of the side force problem. For this problem, the shell is again free of surface load, clamped to a fixed rigid wall at the outer helical edge $r = r_0$ and clamped to a movable rigid cylinder at the inner helical edge $r = r_i$. The rigid cylinder is displaced laterally an amount δ, say in the x-direction. Of interest are the side force P needed to produce this lateral displacement as well as the stress distributions. Evidently, the problem is one with prescribed displacement boundary conditions. Since the displacement components are effectively the integrals of the two primary unknowns ϕ and ψ in our formulation (see Section 6), it appears that the auxiliary conditions supplementing the differential equations would involve integrals of these unknowns across the shell width. We will show that the usual displacement conditions can in fact be transformed into three independent conditions on the values of ϕ and ψ and their derivatives up to second order at each of the two helical edges of the shells and one integral condition. The six edge conditions reduce the problem with prescribed edge displacements to a two point boundary value problem for ϕ and ψ. The solution of this problem determines the stress and strain distributions completely in terms of the resultant side force P, which is related to the lateral displacement δ by the remaining integral condition.

By transforming the prescribed displacement conditions into conditions for ϕ and ψ as described above, we will have established also the fact that the side force problem is the static geometric dual of the problem of pure bending. Therefore, known results for the latter, translated according to the rules of static geometric duality, will become results for the former. Moreover, the computer program developed to solve the pure bending problem can also be used (without any modification) to generate solutions for the side force problem. The procedure is simply to use for the input parameters of the computer program, the values of their dual quantities and to interpret the output values as the results for the dual quantities.

The above use of the static geometric duality of shell theory to avoid duplicating programming effort is not confined to the specific problems considered herein. In fact, any computer program written for a stress boundary value problem of elastic shells can be used to generate the solution for a displacement boundary value problem provided that the stress strain relations possess an inherent static geometric duality (and the generally accepted first approximation stress strain relations for elastic shells do) and provided that we properly reformulate the displacement boundary conditions in terms of the strain and curvature change measures. The latter is always possible in view of the results of [10].

2. Formulation of the pure bending problem

To effect a finite difference solution of equations (1.2) and the associated boundary conditions for the pure bending problem, we introduce the dimensionless variables

$$\rho = \frac{r}{r_0}, \qquad \rho_i = \frac{r_i}{r_0}, \qquad \lambda = \frac{r_0}{a}, \qquad \mu^3 = \frac{2a}{\sqrt{DA}} \frac{r_0^3}{(a^2 + r_0^2)^{3/2}} \tag{2.1}$$

$$\Phi = \frac{\phi}{k}, \qquad \Psi = \sqrt{\frac{A}{D}} \frac{\psi}{k} \tag{2.2}$$

In the absence of surface load and resultant side force so that $P = 0$, the two differential equations (1.2) may be written in dimensionless form

$$\Psi^{\cdots} + \frac{6\lambda^2\rho}{1+\lambda^2\rho^2}\Psi^{\cdot\cdot} + \frac{(7+\nu_s)\lambda^2 + 3\lambda^4\rho^2}{(1+\lambda^2\rho^2)^2}\Psi^{\cdot} - \frac{(8-\nu_s)\lambda^4\rho + 3\lambda^6\rho^3}{(1+\lambda^2\rho^2)^3}\Psi + \mu^3\left(\frac{1+\lambda^2}{1+\lambda^2\rho^2}\right)^{3/2}\Phi = 0 \tag{2.3}$$

$$\Phi^{\cdots} + \frac{6\lambda^2\rho}{1+\lambda^2\rho^2}\Phi^{\cdot\cdot} + \frac{(7-\nu_b)\lambda^2 + 3\lambda^4\rho^2}{(1+\lambda^2\rho^2)^2}\Phi^{\cdot} - \frac{(8+\nu_b)\lambda^4\rho + 3\lambda^6\rho^3}{(1+\lambda^2\rho^2)^3}\Phi + \mu^3\left(\frac{1+\lambda^2}{1+\lambda^2\rho^2}\right)^{3/2}\Psi = \frac{(3-\nu_b)\lambda^3}{(1+\lambda^2\rho^2)^3} \tag{2.4}$$

where dots indicate differentiation with respect to ρ.

For the pure bending problem, the helical edges are free of edge traction so that $N_r + M_{r\theta}/R = N_{r\theta} = M_r = Q_r + (1/\alpha)(\partial M_{r\theta}/\partial\theta) = 0$ at $r = r_i, r_0$ where $R = \alpha^2/a$ is the torsional radius of curvature of the undeformed middle surface of the shell. Since there is no resultant edge force at the two radial edges $\theta = \pm\theta_0$, overall force equilibrium requires that [4]

$$\alpha n_r + r n_{r\theta} - a q_r = Pa = 0 \tag{2.5}$$

Therefore, the four homogeneous Kirchhoff–Bassett stress boundary conditions are only three independent conditions. We take them to be

$$r = r_i, r_0: \qquad n_{r\theta} = m_r = q_r + m/\alpha = 0 \tag{2.6}$$

The parameter k is related to the applied moment M_p (turning about the x-axis) at the radial edges by the integral relation [4]

$$M_p = -\int_{r_i}^{r_0} m_\theta \, dr \tag{2.7}$$

To transform the conditions (2.6) and (2.7) into conditions for Φ and Ψ, we need the expressions for the stress resultants and couples in terms of the stress and strain function. The exact expressions contain many negligible terms [3]; we will list here only the dimensionless form of the simplified expressions with all negligible terms omitted:

$$\sqrt{\frac{A}{D}}\frac{n_\theta}{k} = -\frac{\sqrt{1+\lambda^2\rho^2}}{\lambda}\left(\Psi^\cdot + \frac{2\lambda^2\rho}{1+\lambda^2\rho^2}\Psi\right), \qquad \sqrt{\frac{A}{D}}\frac{n_r}{k} = -\frac{\lambda\rho}{1+\lambda^2\rho^2}\Psi$$

$$\sqrt{\frac{A}{D}}\frac{n_{r\theta}}{k} = \Psi \simeq \sqrt{\frac{A}{D}}\frac{n_{\theta r}}{k}, \qquad \frac{m}{Dk} = (1-\nu_b)\Phi$$

$$\frac{m_r}{Dk} = -\frac{\sqrt{1+\lambda^2\rho^2}}{\lambda}\left[\Phi^\cdot + \frac{(2+\nu_b)\lambda^2\rho}{1+\lambda^2\rho^2}\Phi + \frac{\nu_b\lambda}{1+\lambda^2\rho^2}\right]$$

$$\frac{m_\theta}{Dk} = -\frac{\sqrt{1+\lambda^2\rho^2}}{\lambda}\left[\nu_b\Phi^\cdot + \frac{(1+2\nu_b)\lambda^2\rho}{1+\lambda^2\rho^2}\Phi + \frac{\lambda}{1+\lambda^2\rho^2}\right] \tag{2.8}$$

$$\frac{r_0 q_r}{Dk} = -\frac{\sqrt{1+\lambda^2\rho^2}}{\lambda}\left[\Phi^{\cdot\cdot} + \frac{4\lambda^2\rho}{1+\lambda^2\rho^2}\Phi^\cdot + \frac{3\lambda^2}{(1+\lambda^2\rho^2)^2}\Phi - \frac{\lambda^3\rho}{(1+\lambda^2\rho^2)^2}\right]$$

$$\frac{r_0 q_\theta}{Dk} = \Phi^\cdot + \frac{3\lambda^2\rho}{1+\lambda^2\rho^2}\Phi + \frac{\lambda}{1+\lambda^2\rho^2}\left[1 - \frac{2(3-\nu_b)}{1+\lambda^2\rho^2}\right]$$

With the help of (2.8), the boundary conditions (2.6) become

$$\rho = \rho_i, 1: \qquad \Psi = 0, \qquad \Phi^\cdot + \frac{(2+\nu_b)\lambda^2\rho}{1+\lambda^2\rho^2}\Phi + \frac{\nu_b\lambda}{1+\lambda^2\rho^2} = 0$$

$$\Phi^{\cdot\cdot} + \frac{4\lambda^2\rho}{1+\lambda^2\rho^2}\Phi^\cdot + \frac{(2+\nu_b)\lambda^2 - (1-\nu_b)\lambda^4\rho^2}{(1+\lambda^2\rho^2)^2}\Phi - \frac{\lambda^3\rho}{(1+\lambda^2\rho^2)^2} = 0 \tag{2.9}$$

and the integral condition (2.7) becomes

$$M_p = Dka\int_{\rho_i}^{1}\left[\nu_b\Phi^\cdot + \frac{(1+2\nu_b)\lambda^2\rho}{1+\lambda^2\rho^2}\Phi + \frac{\lambda}{1+\lambda^2\rho^2}\right]\sqrt{1+\lambda^2\rho^2}\,d\rho \equiv Bk \tag{2.10}$$

The two coupled ordinary differential equations (2.3) and (2.4) and the boundary conditions (2.9) define a two point boundary value problem for Φ and Ψ. Upon substituting the solution for Φ into (2.10), we obtain a linear relation between the applied moment, M_p, and the curvature of the axis of the helicoid after deformation.

For the two extreme cases $\lambda^2 \ll 1$ and $(\lambda\rho_{\min})^2 \gg 1$, the solution for the above pure bending problem has been obtained for all μ [4, 5, 9]. Also, for the extreme case $\mu \gg 1$, an asymptotic solution was given in [4] for all λ. We will obtain in the next two sections a finite difference solution valid for all λ and μ. Numerical results not covered by previous solutions will be given in Section 4, in particular, for shells with both λ and μ of order unity and for shells with $\lambda \gg 1$ but $|\lambda\rho|_{\min}$ not large compared to unity. An important special case of the latter is a highly pretwisted strip for which $\rho_i = -1$ and $|\lambda\rho|_{\min} = 0$. Note that we allow the radial coordinate r to take on negative values in order to simplify the specification of a pretwisted strip. By a point (r, θ, z) with $r < 0$, we mean the point $(|r|, \theta + \pi, z)$.

Finally, the strain and curvature change measures are obtained from stress resultants and couples by way of the stress strain relations

$$e_r = A(n_r - \nu_s n_\theta), \qquad e_\theta = A(n_\theta - \nu_s n_r), \qquad e = A_s(n_{r\theta} + n_{\theta r}) \tag{2.11}$$

$$m_\theta = D(k_\theta + \nu_b k_r), \qquad m_r = D(k_r + \nu_b k_\theta), \qquad m = D_s(k_{\theta r} + k_{r\theta}) \tag{2.12}$$

where $D_s = \frac{1}{2}(1 - \nu_b)D$ and $A_s = \frac{1}{2}(1 + \nu_s)A$. The middle surface displacement components are then obtained from the strain and curvature change measures in a manner to be described in Section 6.

3. A staggered mesh difference scheme

To obtain a finite difference solution of the two point boundary value problem defined by (2.3), (2.4) and (2.9), we note that the usual central difference scheme leads to an inconsistent finite difference analog of the differential equations. To see this, consider the difference analog of the simpler pair of the equations

$$u^{\cdots} + \mu^3 v = 0, \qquad v^{\cdots} + \mu^3 u = 0 \qquad (\rho_i < \rho < 1) \tag{3.1, 2}$$

based on a second order central difference scheme with an equally spaced mesh. With $\rho_k = \rho_i + kt, k = 0, 1, 2, \ldots, m, u_k = u(\rho_k)$ and $v_k = v(\rho_k)$, we have for such a scheme,

$$\begin{aligned} u_k^{\cdot} &\cong \frac{1}{2t}(u_{k+1} - u_{k-1}), \qquad u_k^{\cdot\cdot} \cong \frac{1}{t^2}(u_{k+1} - 2u_k + u_{k-1}) \\ u_k^{\cdots} &\cong \frac{1}{2t^3}(u_{k+2} - 2u_{k+1} + 2u_{k-1} - u_{k-2}) \end{aligned} \tag{3.3}$$

and analogous formulas for v, where $t = (1 - \rho_i)/m$. The finite difference analog of (3.1) and (3.2) is then

$$\begin{aligned} u_{k+2} - 2u_{k+1} + 2u_{k-1} - u_{k-2} + 2(\mu t)^3 v_k &= 0 \\ v_{k+2} - 2v_{k+1} + 2v_{k-1} - v_{k-2} + 2(\mu t)^3 u_k &= 0 \end{aligned} \tag{3.4}$$

The coupled difference equations (3.4) have constant coefficients and thus solutions proportional to β^k where β is a root of the eight degree polynomial

$$(\beta^4 - 2\beta^3 + 2\beta - 1)^2 - (2\mu^3 t^3)^2 \beta^4 = 0 \tag{3.5}$$

Thus, v_k and u_k have eight linearly independent solutions. For $\mu t \ll 1$, we have except for higher order terms in (μt)

$$\beta_n = 1 + \mu t\, e^{in\pi/3}, \qquad (n = 1, 2, \ldots, 6), \qquad \beta_{7,8} = -1 + \tfrac{1}{4}\mu^3 t^3 \tag{3.6}$$

The solutions corresponding to the first six roots tend to the six linearly independent solutions of the exact system (3.1) and (3.2) as $t \to 0$. Evidently, β_7 and β_8 lead to spurious solutions for the original system of differential equations. As such, the difference scheme leads to an inconsistent difference analog for (3.1) and (3.2). An approximate solution of the boundary value problem by way of this naive difference scheme will not in general converge to the exact solution.

We can, of course, reduce the system (3.1) and (3.2) to a single sixth order equation for u or v and the same central difference scheme (with corresponding difference formulas for f^{iv}, f^{v} and f^{vi}) will give a consistent finite difference analog of this sixth order equation. However, the physical problem dictates that we should deal with the system (3.1) and (3.2) directly since we would like to retain the option of setting $\mu = 0$ in which case the system decouples. In the actual problem, $\mu = 0$ corresponds to the limiting case of a helicoidal shell with zero pitch (a flat plate) so that the bending and stretching actions decouple.

To handle (3.1) and (3.2) directly, we will use a difference scheme based on the concept of staggered mesh. First, we halve the mesh size so that $t = (1 - \rho_i)/2m$ and introduce two additional points with the same spacing beyond each of the two end points so that $k = -2, -1, \ldots, 2m + 2$. Next, we define u and v only on the odd and even mesh points, respectively, and denote them by U_k (k odd) and V_k (k even). With the difference approximations

$$f_k = \frac{1}{2}(f_{k+1} + f_{k-1}) + 0(t^2), \qquad \dot{f}_k = \frac{1}{2t}(f_{k+1} - f_{k-1}) + 0(t^2)$$

$$\ddot{f}_k = \frac{1}{8t^2}(f_{k+3} - f_{k+1} - f_{k-1} + f_{k-3}) + 0(t^2) \tag{3.7}$$

$$\dddot{f}_k = \frac{1}{8t^3}(f_{k+3} - 3f_{k+1} + 3f_{k-1} - f_{k-3}) + 0(t^2)$$

obtained from Taylor's theorem, we write a difference equation corresponding to (3.1) at each of the even interior points and a difference equation corresponding to (3.2) at each of the odd interior points. We get then

$$\begin{aligned} &U_{k+3} - 3U_{k+1} + 3U_{k-1} - U_{k-3} + (\mu t)^3 V_k = 0 \qquad (k = 2, 4, \ldots, 2m-2) \\ &V_{k+3} - 3V_{k+1} + 3V_{k-1} - V_{k-3} + (\mu t)^3 U_k = 0 \qquad (k = 1, 3, \ldots, 2m-1) \end{aligned} \tag{3.8}$$

The solutions of (3.8) are of the form $U_k = c_1\beta^{k/2}$ and $V_k = c_2\beta^{k/2}$ where β is a root of the sixth degree polynomial

$$(\beta^3 - 3\beta^2 + 3\beta - 1)^2 - (\mu t)^6\beta^3 = 0 \tag{3.9}$$

Except for higher order terms in μt, we have

$$\beta_n = 1 + \mu t\, e^{n\pi i/3} \qquad (n = 1, 2, \ldots, 6) \tag{3.10}$$

As $t \to 0$, the six linearly independent finite difference solutions tend to the six exact linearly independent solutions of (3.1) and (3.2) and there is no spurious solution associated with this difference analog.

We will use this staggered mesh scheme for the pure bending problem formulated in the last section with Ψ and Φ taking the place of u and v, respectively. The difference equations for Ψ_k (k odd) and Φ_k (k even) corresponding to (3.8) have variable coefficients and consist of $(2m - 1)$ linear algebraic equations for $2m + 5$ unknowns, Φ_{-2}, Ψ_{-1}, Φ_0, $\Psi_{1,\ldots}$, Ψ_{2m+1}, Φ_{2m+2}. The six additional equations needed to complete the system are supplied by the boundary conditions (2.9).

With the help of (3.7), these boundary conditions become

$$\Psi_{k-1} + \Psi_{k+1} = 0, \qquad \Phi_{k+2} - \Phi_{k-2} + 4t\left[\frac{\lambda^2\rho_k(2+\nu_b)}{1+\lambda^2\rho_k^2}\Phi_k + \frac{\nu_b\lambda}{1+\lambda^2\rho_k^2}\right] = 0$$

$$\Phi_{k+2} - 2\Phi_k + \Phi_{k-2} + \frac{4t\lambda^2\rho_k}{1+\lambda^2\rho_k^2}(\Phi_{k+2} - \Phi_{k-2}) + \frac{4t^2}{(1+\lambda^2\rho_k^2)^2}[(2+\nu_b)\lambda^2 - (1-\nu_b)\lambda^4\rho_k^2]\Phi_k - \frac{4t^2\lambda^3\rho_k}{(1+\lambda^2\rho_k^2)^2} = 0 \tag{3.11}$$

for $k = 0$ and $k = 2m$.

The solution Φ_k (k even) and Ψ_k (k odd) of this system is then used in conjunction with (3.7) and (2.8) to obtain the stress distribution* and in (2.10) to get the stiffness coefficient B.

Solutions of the difference equations for Φ_k (k even) and Ψ_k (k odd) have been obtained for different combinations of ρ_i, λ, ν and $\gamma = h/r_0$ though only results for $\nu = 0.3$ will be presented here. A mesh with $m = 200$ was used in most cases, however, convergence is often achieved with $m = 100$. Double precision arithmetic was used so that no significant round-off error would occur even for a very fine mesh.

The finite difference solution was tested against the available shallow shell solutions [4, 5, 9] and asymptotic solution [4]. The results are in excellent agreement with the shallow shell solution for $\lambda \lesssim 0.2$ and $(\lambda\rho_{\min})^{-1} \lesssim 0.2$ and with the asymptotic solution for $\mu \geq 10$.

4. Pure bending of a pretwisted strip

The behavior of a helicoidal shell under the action of end bending moments depends on the geometrical parameters ρ_i, λ and μ and the material parameters $\nu(= \nu_s = \nu_b)$ and E (which appears only as a scale factor). We will fix $\nu = 0.3$ for all the results presented herein. The parameter μ depends on the width to pitch ratio, $\lambda = r_0/a$, and the width-to-thickness ratio, $\gamma = r_0/h$, with the latter always large compared to unity. For a homogeneous and isotropic shell, we have from (1.3) and (2.2) that

$$\mu^3 = 0\left[\frac{\gamma\lambda^2}{(1+\lambda^2)^{3/2}}\right] \tag{4.1}$$

For a fixed value of $\gamma \gg 1$, μ first increases from zero and then decreases to zero as λ increases from zero to infinity. The behavior of μ as a function of γ and λ is given in Figure 1. From the structure of the differential equations (2.3) and (2.4), it is clear that the behavior of the shell is qualitatively different for $\mu \gg 1$ and $\mu = 0(1)$. The asymptotic solution obtained in [4] shows that there is an edge zone phenomenon for $\mu \gg 1$.

* Expressions for stress measures which are exact to within the error inherent in a first approximation shell theory were used instead of (2.8) in [3].

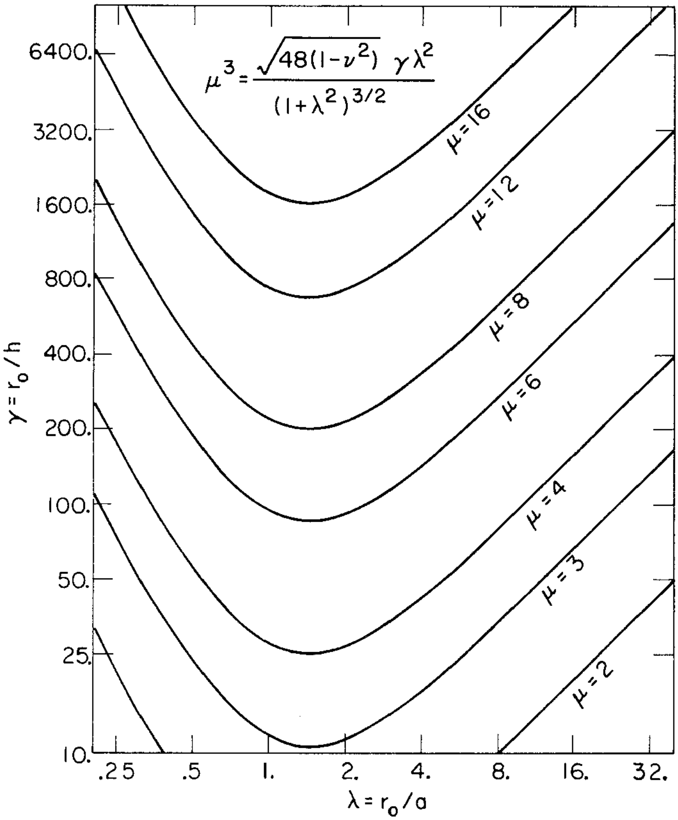

Figure 1. Contour lines of a dimensionless edge zone width parameter μ.

It should be noted that for shell theory to be applicable, we must have

$$\frac{h}{R_{\min}} = \left[\frac{ah}{a^2 + r_{\min}^2}\right] \ll 1 \tag{4.2}$$

where $R_{\min}$ and $r_{\min}$ are the minimum torsional radius of curvature and the minimum radial distance from the axis of the helicoid to points of the shell, respectively. For a pretwisted strip ($r_i = -r_0$), we have $r_{\min} = 0$ and therefore

$$\frac{h}{R_{\min}} = 0\left(\frac{h}{a}\right) \tag{4.3}$$

no matter how small the pitch parameter a may be. Consequently, for a fixed value of h, a cannot be too small in this case if shell theory is to remain applicable to the pretwisted strip.

For the limiting case of a flat strip ($\lambda = 0, \theta_0 = 0$ and $\rho_i = -1$), the stiffness relation (2.10) and the only nonvanishing stress quantity are known to be [4]:

$$M_p = 2r_0 D(1 - \nu^2)k \equiv B_{0s}k, \qquad \sigma_{\theta B} = \frac{6M_\theta}{h^2} = -\frac{3M_p}{r_0 h^2} \equiv -\sigma_{0B} \tag{4.4}$$

As λ increases from zero but within the range $0 < \lambda \ll \gamma^{-1/2}$ (so that $\mu^3 \ll 1$), the stiffness relation and the stress state of the shell differ from the flat plate solution (4.4) only by higher order terms in λ and/or μ [4]. For larger values of λ in the range $\gamma^{-1/2} \ll \lambda \ll \gamma$ (the second half of the inequality is dictated by the condition $h/a \ll 1$), we have $\mu^3 = 0(a/h) \gg 1$. If $(a/h)^{1/3} \gg 1$, the asymptotic solution obtained in [4] gives, except for $0(\mu^{-1})$ terms,

$$M_p \sim kDa \ln\left[\frac{\sqrt{1+\lambda^2}+\lambda}{\sqrt{1+\lambda^2}-\lambda}\right] \equiv kB_I \tag{4.5}$$

and the corresponding stress measures.

Since λ must be much smaller than γ for the use of shell theory for a pretwisted strip, it remains only to study the solution for $\gamma^{-1/2} \lesssim \lambda \ll \gamma$ with $\mu = 0(1)$. The solution for this range of λ can now be obtained by the finite difference scheme of Section 3.

A plot of B/B_{0s} is given in Figure 2 for several values of λ over the entire range of λ, though only that portion for which $h/a = \lambda/\gamma \ll 1$ should be used. From these results, we see that the overall bending stiffness of moderately thin shells is smaller than the corresponding flat strip stiffness and is monotone decreasing function of λ.

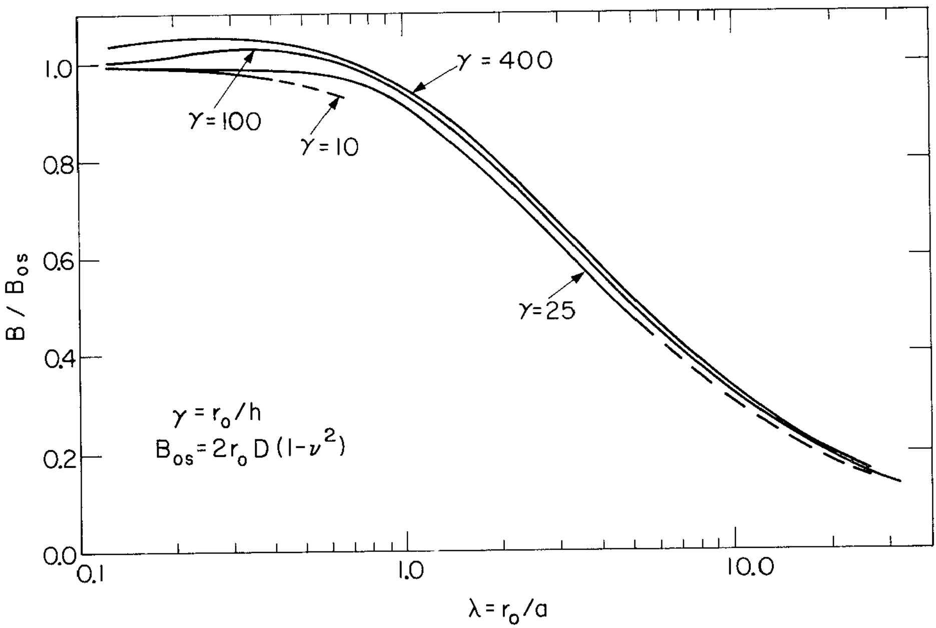

Figure 2. Overall bending stiffness of pretwisted strips.

For very thin shells, the same stiffness increases slightly from the flat strip value with λ but eventually decreases below the flat strip stiffness and tends to the asymptotic value given by (4.5). These observations are in agreement with the qualitative behavior suggested by the perturbation ($\mu^3 \ll 1$) and asymptotic ($\mu \gg 1$) solution.

Since $\gamma \gg 1$ for shells, the range $\lambda^2 = 0(\gamma^{-1})$ can be treated by shallow shell theory (see [4, 5]). Therefore, plots of representative bending and direct stresses given in Figures 3 and 4 are only given for the $\lambda \gg \gamma^{-1/2}$ and $\mu = 0(1)$ range. The results for $\lambda = 0$ are also included as a reference state.

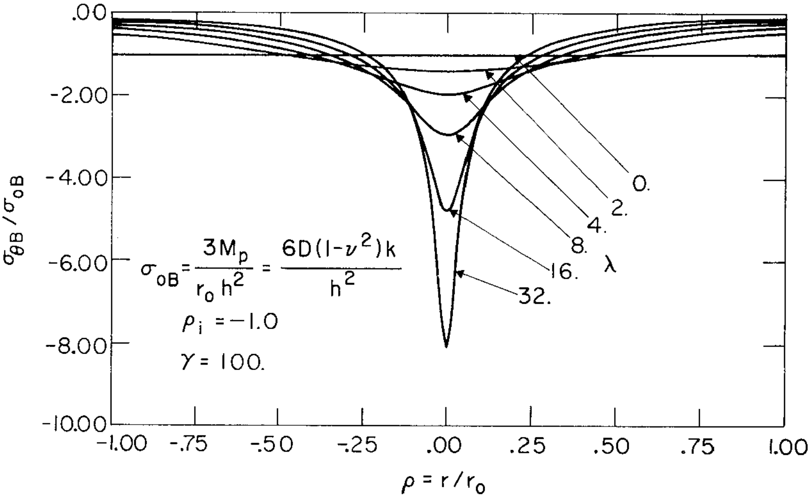

Figure 3. Tangential bending stress distribution in pretwisted strips in pure bending. ($\theta = 0$).

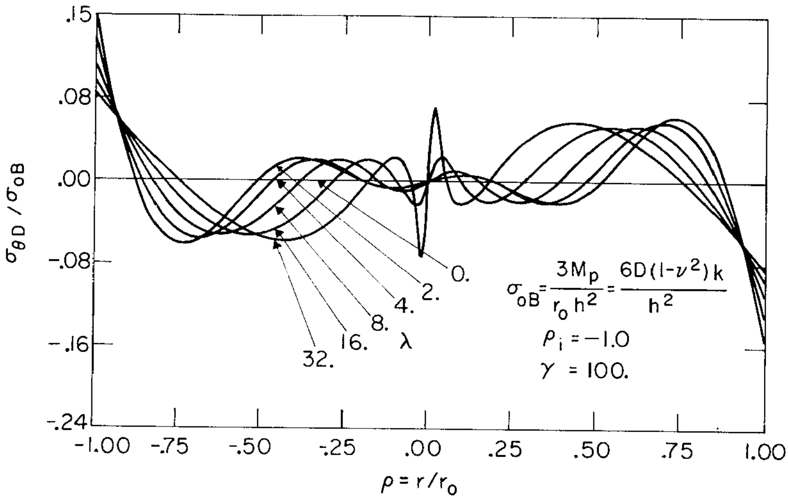

Figure 4. Tangential direct stress distribution in pretwisted strips in pure bending. ($\theta = \pi/2$).

From Figure 3, we see that the bending stress $\sigma_{\theta B}$ exhibits a stress concentration phenomenon for large values of λ. This is reminiscent of the corresponding phenomenon found in [8] for the problem of axial torsion and extension.

Finally, the plots for the direct stress $\sigma_{\theta B}$ given in Figure 4 show an edge effect when $\mu \gg 1$ as predicted by the asymptotic solution. The minimum boundary layer width occurs at about $\lambda = 1$. Note that the direct stress is an order of magnitude smaller than the bending stress in the range of λ and γ considered

5. Pure bending of a coreless shell

In cases where $\rho_i > 0$, we have for the limiting case of a flat rectangular plate ($\lambda = 0$ and $\theta_0 = 0$)

$$M_p = kD(1 - \nu^2)(r_0 - r_i) \equiv B_0 k, \qquad \sigma_{\theta B} = -\frac{6M_p}{h^2}\frac{1}{r_0 - r_i} \tag{5.1}$$

For $0 < \lambda \ll \gamma^{-1/2}$, the stiffness relation and the stress state of the shell differ from the plate solution (5.1) again only by higher order terms in λ and/or μ^{-1} [4]. For larger values of λ in the range $\gamma^{-1/2} \ll \lambda \ll \gamma$, the asymptotic solution obtained in [4] gives, except for $0(1/\mu)$ terms,

$$M_p \sim kDa \ln\left[\frac{\sqrt{1 + \lambda^2} + \lambda}{\sqrt{1 + \lambda^2\rho_i^2} + \lambda\rho_i}\right] \equiv B_I k \tag{5.2}$$

But, unlike the case $|\rho|_{\min} = 0$, we have now the limiting case of a circular ring plate sector when $a = 0$. From plate theory (see [9] and references therein), we have

$$M_p = \frac{kaD(1 - \nu_b)}{4(3 + \nu_b)}\left[(3 + \nu_b)^2 \ln \rho_i + \frac{(1 - \nu_b)^2(1 - \rho_i^2)}{1 + \rho_i^2}\right] \equiv B_\infty k_\infty . \tag{5.3}$$

where $k_\infty \equiv ka$ must be kept finite as $a \to 0$. For shells with a small pitch-to-width ratio so that $0 < \lambda^{-1} \ll \gamma^{-1/2}$ (and therefore $\mu^3 \ll 1$), the overall bending stiffness and the stress state of the shell differ from those of the circular ring plate sector only by higher order terms in λ^{-1} and μ [4].

For the range of γ and μ not covered by the above solutions, extensive numerical results have obtained in [3] by the finite difference scheme of section (3).

6. Multivalued displacement field

The displacement field associated with our class of problems is of the form [8]

$$\begin{aligned} u(r, \theta) &= U(r)\sin\theta + \frac{ka^2}{4}[(1 + \theta^2)\sin\theta - \theta\cos\theta] \\ v(r, \theta) &= V(r)\cos\theta - \frac{ka^2 r}{4\alpha}[\theta\sin\theta - \theta^2\cos\theta] \\ w(r, \theta) &= W(r)\cos\theta - \frac{ka}{4\alpha}[a^2\theta^2\cos\theta + (a^2 + 2r^2)\theta\sin\theta] \end{aligned} \tag{6.1}$$

where u, v and w are the radial, tangential and normal component of the midsurface displacement vector respectively, and where U, V and W are to be determined from the reduced strain displacement relations [8]

$$e_r = U', \qquad e_\theta = \frac{rU}{\alpha^2} - \frac{V}{\alpha}$$

$$e_{r\theta} = V' + \frac{W}{R} - \Omega, \qquad e_{\theta r} = \frac{U}{\alpha} - \frac{rV}{\alpha^2} + \frac{W}{R} + \Omega$$

$$k_r = \Phi_r' + \frac{\Omega}{R}, \qquad k_{r\theta} = \Phi_\theta', \qquad l_r = \Omega' - \frac{\Phi_r}{R} \tag{6.2}$$

$$k_\theta = \frac{r\Phi_r}{\alpha^2} + \frac{\Phi_\theta}{\alpha} - \frac{a\Omega}{\alpha^2} + \frac{ka}{\alpha}, \qquad k_{\theta r} = -\frac{\Phi_r}{\alpha} - \frac{r\Phi_\theta}{\alpha^2}, \qquad l_\theta = -\frac{\Omega}{\alpha} + \frac{\Phi_\theta}{R}$$

with

$$\Phi_\theta = \frac{W}{\alpha} + \frac{U}{R}, \qquad \Phi_r = -W' + \frac{V}{R}, \qquad \Omega = \frac{1}{2\alpha}[(\alpha V)' - U] \tag{6.3}$$

where primes indicate differentiation with respect to r. Note that $e_{r\theta} = e_{\theta r} = e$. These expressions reveal an algebraic compatibility equation of the form

$$\alpha k_\theta + r k_{\theta r} - a l_\theta = ka \tag{6.4}$$

which is a first integral of the differential equation of compatibility obtained in [2, 3, 4] as a static geometric dual of the first integral of the differential equations of equilibrium (2.5).

With the r-dependent portion of the strain and curvature change measures completely determined once we have ϕ and ψ, the displacement components can be determined by integrating the system of first order differential equations (6.2), keeping in mind that the compatability equations have already been satisfied identically in our formulation [4]. We give here the solution for U, V and W in a form suitable for our purpose:

$$U = \int^r e_r\, dr, \qquad V = -\alpha\, e_\theta + \frac{r}{\alpha} U,$$

$$W = \frac{r\alpha}{2a} e_\theta + \frac{\alpha^3}{2a}\left(l_\theta + \frac{e}{\alpha}\right) + \frac{a}{\alpha} U, \tag{6.5}$$

$$\Phi_r = -\alpha k_{\theta r} - \frac{r}{\alpha^2}\left(\frac{a}{\alpha} U + W\right), \qquad \Phi_\theta = \frac{W}{\alpha} + \frac{U}{R}, \qquad \Omega = -\alpha l_\theta + \frac{a}{\alpha}\Phi_\theta$$

7. Formulation of the side force problem

The boundary conditions for the side force problem at the two helical edges are evidently prescribed in terms of the displacement components in the form

$$r = r_0: \qquad u = v = w = \frac{\partial w}{\partial r} = 0 \tag{7.1}$$

$$r = r_i: \qquad u = \delta \sin\theta, \qquad v = \frac{r\delta}{\alpha}\cos\theta,$$

$$w = -\frac{a\delta}{\alpha}\cos\theta, \qquad \frac{\partial w}{\partial r} = \frac{ra\delta}{\alpha^3}\cos\theta \tag{7.2}$$

In terms of U, V, W, and Φ_r, they become

$$r = r_0: \qquad U = V = W = \Phi_r = 0 \tag{7.3}$$

$$r = r_i: \qquad U = \delta, \quad V = \frac{r\delta}{\alpha}, \quad W = -\frac{a\delta}{\alpha}, \quad \Phi_r = 0 \tag{7.4}$$

From the expressions given by (6.5), it is not difficult to verify that (7.3) and (7.4) (along with $k = 0$) are in turn equivalent to

$$r = r_i, r_0: \qquad k_{\theta r} = e_\theta = l_\theta + \frac{e}{\alpha} = 0 \tag{7.5}$$

and

$$-\int_{r_i}^{r_0} e_r \, dr = \delta \tag{7.6}$$

Thus, the side force problem is effectively reduced to a two point boundary value problem consisting of two coupled ODE (1.2) (with $k = 0$ and $P \neq 0$) and three independent boundary conditions (7.5) at each of the two helical edges. The resultant side force per unit axial length, P, is then related to the lateral displacement δ by (7.6).

With $\hat{\Psi} = \psi/P$ and $\hat{\Phi} = \sqrt{D/A}(\phi/P)$, the two governing differential equations may be written in dimensionless form

$$\begin{aligned}\hat{\Psi}^{\cdots} &+ \frac{6\lambda^2\rho}{1+\lambda^2\rho^2}\hat{\Psi}^{\cdot\cdot} + \frac{(7+\nu_s)\lambda^2 + 3\lambda^4\rho^2}{(1+\lambda^2\rho^2)^2}\hat{\Psi}^{\cdot} - \frac{(8-\nu_s)\lambda^4\rho + 3\lambda^6\rho^3}{(1+\lambda^2\rho^2)^3}\hat{\Psi} \\ &+ \mu^3\left(\frac{1+\lambda^2}{1+\lambda^2\rho^2}\right)^{3/2}\hat{\Phi} = \frac{(3+\nu_s)\lambda^3}{(1+\lambda^2\rho^2)^3}\end{aligned} \tag{7.7}$$

$$\begin{aligned}\hat{\Phi}^{\cdots} &+ \frac{6\lambda^2}{1+\lambda^2\rho^2}\hat{\Phi}^{\cdot\cdot} + \frac{(7-\nu_b)\lambda^2 + 3\lambda^4\rho^2}{(1+\lambda^2\rho^2)^2}\hat{\Phi}^{\cdot} - \frac{(8+\nu_b)\lambda^4\rho + 3\lambda^6\rho^3}{(1+\lambda^2\rho^2)^3}\hat{\Phi} \\ &+ \mu^3\left(\frac{1+\lambda^2}{1+\lambda^2\rho^2}\right)^{3/2}\hat{\Psi} = 0\end{aligned} \tag{7.8}$$

To the same degree of approximation as in (2.8), the expressions for e_r, e_θ, etc. for the present problem are just the static geometric duals of (2.8). That is, we can obtain them from (2.8) by replacing all quantities in (2.8) by their static geometric duals according to the following table*

n_r	n_θ	$n_{r\theta}$	$n_{\theta r}$	q_r	q_θ	m_r	m_θ	m
k_θ	k_r	$k_{\theta r}$	$k_{r\theta}$	l_θ	l_r	e_θ	e_r	e

Φ	Ψ	D	ν_s	k	M_p
$\hat{\Psi}$	$\hat{\Phi}$	A	$-\nu_b$	P	δ

In particular, the boundary conditions (7.5) can be expressed in terms of $\hat{\Phi}$ and $\hat{\Psi}$ as

$$\begin{aligned}\rho = \rho_i, 1: \qquad &\hat{\Phi} = 0, \quad \hat{\Psi}^{\cdot} + \frac{(2-\nu_s)\lambda^2\rho}{1+\lambda^2\rho^2}\hat{\Psi} - \frac{\nu_s\lambda}{1+\lambda^2\rho^2} = 0 \\ &\hat{\Psi}^{\cdot\cdot} + \frac{4\lambda^2\rho}{1+\lambda^2\rho^2}\hat{\Psi}^{\cdot} + \frac{(2-\nu_s)\lambda^2 - (1+\nu_s)\lambda^4\rho^2}{(1+\lambda^2\rho^2)^2}\hat{\Psi} - \frac{\lambda^3\rho}{(1+\lambda^2\rho^2)^2} = 0\end{aligned} \tag{7.9}$$

* Note that we display here the duality between the r dependent parts of the stress and strain resultants rather than between the resultants themselves.

and the integral relation (7.6) can be expressed as

$$\delta = PAa \int_{\rho_i}^{1} \left[-\nu_s \hat{\Psi}^{\cdot} + \frac{(1 - 2\nu_s)\lambda^2 \rho}{1 + \lambda^2 \rho^2} \hat{\Psi} + \frac{\lambda}{1 + \lambda^2 \rho^2} \right] \sqrt{1 + \lambda^2 \rho^2}\, d\rho \equiv \hat{B} P \tag{7.10}$$

The solution of the boundary value problem (7.7), (7.8) and (7.9) can be obtained by methods used for the pure bending problem. But, since the differential equations (7.7) and (7.8), the "strain" boundary conditions (7.9) and the flexibility relation (7.10) are the static geometric duals of the differential equations (2.4) and (2.3), the stress boundary conditions (2.9) and the stiffness relation (2.10), we can take advantage of the complete static geometric duality of the two problems and obtain the solution of the side force problem directly from the solution of the pure bending problem. For example, since

$$\hat{B}(A, \nu_s, \nu_b) \leftrightarrow B(D, -\nu_b, -\nu_s) \tag{7.11}$$

we have from the asymptotic expression (5.2) for $\mu \gg 1$

$$\delta \sim PAa \ln \left[\frac{\sqrt{1 + \lambda^2} + \lambda}{\sqrt{1 + \lambda^2 \rho_i^2} + \lambda \rho_i} \right] \equiv \hat{B}_M P \tag{7.12}$$

without any additional calculation whatsoever.

Similarly, the finite difference solution for the side force problem can be obtained from the computer program written for the pure bending problem without any modification. With $\nu_b = \nu_s = \nu$, we only have to use $-\nu$ as input for ν and interpret all the output values as results for the dual quantities as described earlier.

It should be emphasized that the above computational use of the static geometric duality does not depend on the use of the simplified expressions for the stress and strain measures in terms of the stress and strain functions. The complete duality between the two seemingly unrelated physical problems is guaranteed by the duality between the differential equations of equilibrium, the stress strain relations (2.11), the exact stress boundary conditions (2.6) and the exact stiffness relation (2.7) on the one hand, and the differential equations of compatibility, the stress strain relations (2.12), the exact strain boundary conditions (7.5) and the exact flexibility relation (7.6) on the other hand.

8. Numerical results for the side force problem by duality

By static geometric duality, we have from (5.1) and (5.3)

$$\delta = PA(1 - \nu^2)(r_0 - r_1) \equiv \hat{B}_0 P \tag{8.1}$$

for $\lambda = 0$, and

$$\delta = \frac{PaA(1 + \nu_s)}{4(3 - \nu_s)} \left[(3 - \nu_s)^2 \ln \rho_i + \frac{(1 + \nu_s)^2 (1 - \rho_i^2)}{1 + \rho_i^2} \right] \equiv \hat{B}_\infty P_\infty \tag{8.2}$$

for $\lambda = \infty$ where the definition of P, (2.5), requires that $P_\infty \equiv Pa$ be kept finite as $a \to 0$ (see also [11]).

For $0 < \lambda \ll \gamma^{-1/2}$ and $0 < \lambda^{-1} \ll \gamma^{-1/2}$, the overall flexibility coefficient (and the corresponding stress distribution) differs from that given by (8.1) and (8.2), respectively, only by higher order terms in μ and/or λ.

For $\gamma^{-1/2} \ll \lambda \ll \gamma^{1/2}$, the application of the static geometric duality to the asymptotic solution (5.2) for the pure bending problem gives (7.12).

With (8.1) and (8.2) as reference states, the ranges of values of λ for which the solution is still to be obtained are the same as those of pure bending problem for a coreless shell. These solutions can now be obtained from the computer program developed for the pure bending problem and the static geometric duality.

We limit ourselves here to plots of the flexibility coefficients for $\lambda \lesssim 30$ for several values of γ (Figure 5) and plots of peak direct and bending radial stresses for $r_i/r_0 = 0.5$, $\gamma = 100$ and for several values of λ (Figures 6 and 7). Note that the peak bending stresses are comparable to the peak direct stresses in magnitude for the combination of geometrical parameters considered.

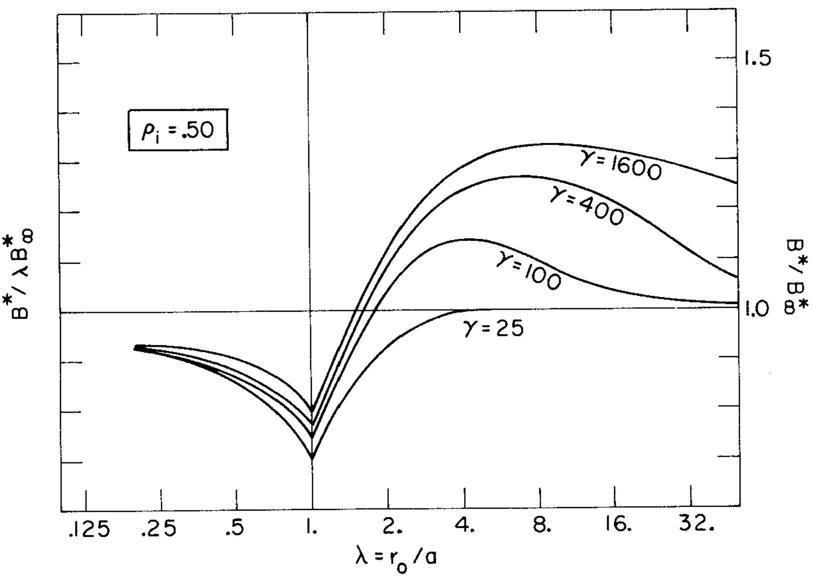

Figure 5. Overall extensional flexibility of helicoidal shells subject to a side force. (See (5.3) for B^*_∞).

References

1. V. S. Chernin, "On the system of differential equations of equilibrium of shells of revolution under bending loads", *P.M.M.* **23**, 258–265 (1959).
2. V. S. Chernin, "First integrals of the static equations and compatibility equations in equilibrium problems for a rectilinear helicoid", Akad. Nauk, SSSR, Izvestia, *Mekhanika Tverdova Tela*, 88–96 (1969).
3. R. L. Mallett, "Circumferentially sinusoidal stress and strain distributions in helicoidal shells", Ph.D. Thesis, *M.I.T.* (Sept. 1970).

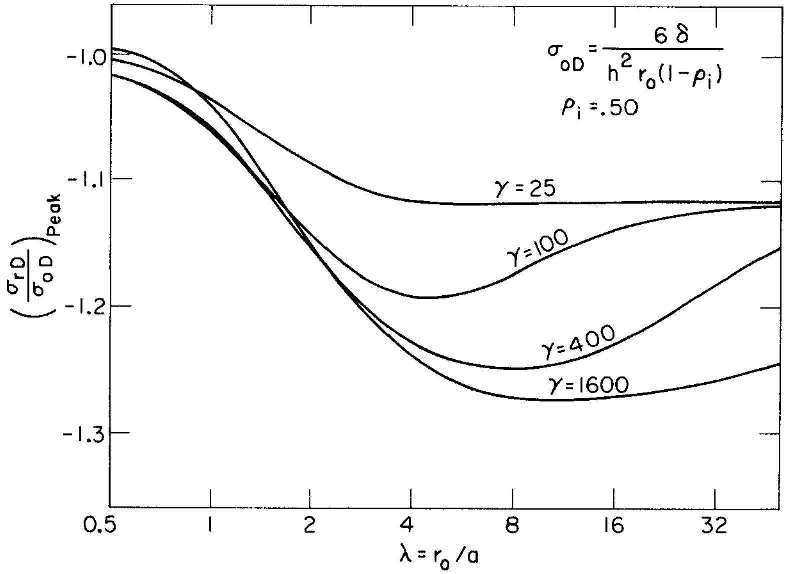

Figure 6. Peak radial direct stress of helicoidal shells subject to a side force.

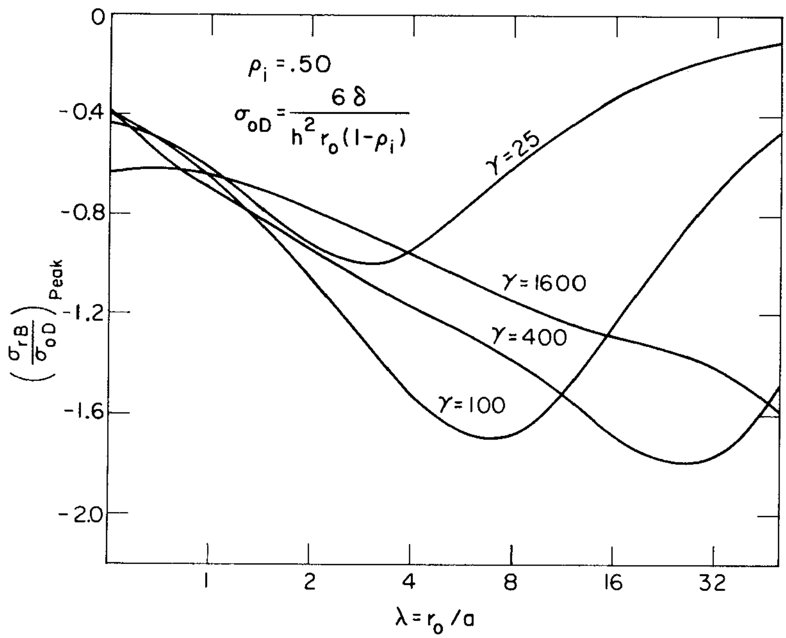

Figure 7. Peak radial bending stress of helicoidal shells subject to a side force.

4. R. L. Mallett and F. Y. M. Wan, "Spirally sinusoidal stress distributions in elastic helicoidal shells", *J. Appl. Math. & Phys.* (*ZAMP*) **22**, 1029–1043 (1971).
5. L. Maunder and E. Reissner, "Pure bending of pretwisted rectangular plates", *J. Mech. Phys. Solids* **5**, 261–266 (1957).
6. E. Reissner, "On the foundations of the theory of elastic shells", *Proc. 11th Intern. Congr. Appl. Mech.* (1964), Springer-Verlag, 20–30 (1966).

7. E. Reissner and F. Y. M. Wan, "On axial extension and torsion of helicoidal shells", *J. Math. and Phys.* **47**, 1–30 (1968).
8. F. Y. M. Wan, "A class of unsymmetric stress distributions in helicoidal shells", *Quart. Appl. Math.* **24**, 374–379 (1967).
9. F. Y. M. Wan, "Pure bending of shallow helicoidal shells", *J. Appl. Mech.* **35**, 387–392 (1968).
10. F. Y. M. Wan, "Two variational theorems for thin shells", *J. Math. and Phys.* **47**, 429–431 (1968).
11. F. Y. M. Wan, "The side force problem for shallow helicoidal shells", *J. Appl. Mech.* **36**, 292–295 (1969).
12. F. Y. M. Wan, "Circumferentially sinusoidal stress distributions in shells of revolution", *Int. J. Solids Structures* **6**, 959–973 (1970).

Stanford University
Massachusetts Institute of Technology

(Received November 20, 1972)